

General Disclaimer

One or more of the Following Statements may affect this Document

- This document has been reproduced from the best copy furnished by the organizational source. It is being released in the interest of making available as much information as possible.
- This document may contain data, which exceeds the sheet parameters. It was furnished in this condition by the organizational source and is the best copy available.
- This document may contain tone-on-tone or color graphs, charts and/or pictures, which have been reproduced in black and white.
- This document is paginated as submitted by the original source.
- Portions of this document are not fully legible due to the historical nature of some of the material. However, it is the best reproduction available from the original submission.

SOUND PROPAGATION IN A DUCT OF PERIODIC WALL STRUCTURE

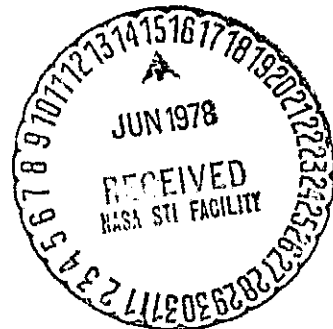
U. Kurze

(NASA-TM-75284) SOUND PROPAGATION IN A DUCT
OF PERIODIC WALL STRUCTURE (National
Aeronautics and Space Administration) 29 F
HC A03/MF A01 CSCI 20A

N78-24901

Unclas
G3/71 21222

Translation of "Schallausbreitung im Kanal mit periodischer
Wandstruktur," Acustica, Vol. 21, No. 2, 1969, pp. 74-85.



1. Report No. NASA TM 75284	2. Government Accession No.	3. Recipient's Catalog No.	
4. Title and Subtitle SOUND PROPAGATION IN A DUCT OF PERIODIC WALL STRUCTURE		5. Report Date May 1978	
		6. Performing Organization Code	
7. Author(s) U. Kurze Bolt, Beranek & Newman, Inc, Cambridge, Mass., USA		8. Performing Organization Report No.	
		10. Work Unit No.	
9. Performing Organization Name and Address Leo Kanner Associates Redwood City, California 94063		11. Contract or Grant No. NASW-2790	
		13. Type of Report and Period Covered Translation	
12. Sponsoring Agency Name and Address National Aeronautics and Space Adminis- tration, Washington, D.C., 20546		14. Sponsoring Agency Code	
15. Supplementary Notes Translation of "Schallausbreitung im Kanal mit periodischer Wandstruktur," Acustica, Vol. 21, No. 2, 1969, pp. 74-85.			
16. Abstract A boundary condition, which accounts for the coupling in the sections behind the duct boundary, is given for the sound-absorbing duct with a periodic structure of the wall lining and using regular partition walls. The soundfield in the duct is suitably described by the method of differences. For locally active walls this renders an explicit approximate solution for the propagation constant. Coupling may be accounted for by the method of differences in a clear manner. Numerical results agree with measurements and yield information which has technical applications.			
17. Key Words (Selected by Author(s))		18. Distribution Statement Unclassified-Unlimited	
19. Security Classif. (of this report) Unclassified	20. Security Classif. (of this page) Unclassified	21. No. of Pages 28	22. Price

SOUND PROPAGATION IN A DUCT OF PERIODIC WALL STRUCTURE¹

U. Kurze

Bolt, Beranek & Newman, Inc., Cambridge, Mass., USA

1. Introduction

174

The duct of periodic wall-structure as a wave guide for acoustic or electromagnetic waves is treated several times in the literature with a transmission theory in which the effect of the periodicity is either ignored by three-dimensional averaging over one period [1] [2] or is to be taken into account by three-dimensional sectioning only in the form of a ladder network [3] [4]. The period, which is determined by the distance between transverse gaps and screens in the duct or resonators and the series of various absorbers and the wall lining, must in the first case be very small with respect to the wavelength. In the second case, the distance between inhomogeneities in the wall of the duct must be large enough in order to be able to describe homogeneous duct sections by the propagation conditions for a basic mode and the higher modes occurring at the inhomogeneities by concentrated elements of a network or reflection and transmission factors of a wave guide.

Both the formation of the average and the ladder network consideration presuppose a locally active duct wall for which the wall conductance as the ratio of the sound particle velocity perpendicular to the wall and the pressure is independent of the field structure of the stimulating sound. The precondition is always met when a sound wave striking the wall is propagated in the wall perpendicular to the plane of the wall. Thus the calculation of homogeneous, sound-absorbing ducts leads to the development of a chamber damper based on a subdivision of the

1. Dissertation excerpt, Berlin Technical University, 1968
*Numbers in the margin indicate pagination in the foreign text.

absorber into very small chambers by means of solid partition walls. In ladder network arrangements the sound propagation which is exclusively perpendicular to the wall can exist in solid porous material between resonators with a small coupling surface in the wall or between screens in the duct.

The technical construction of chamber dampers effective over wide frequency ranges on the one hand does not allow very small chambers because of the cost of material, and on the other hand it does not allow a solid porous absorber on the duct boundary because of the small wall resistance required. It can be seen from the example shown in Fig. 1 how the form

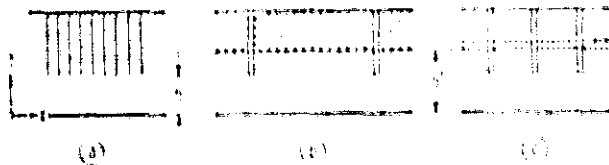


Fig. 1. Model for noise damper calculation.
 (a) homogeneous wall lining
 (b) ladder network
 (c) technical version of the chamber damper.

of practically applicable dampers therefore lies between the limit cases of homogeneous wall lining and ladder network structure. The duct boundary for any arrangement of absorbent material in the chambers is advantageously characterized by means of a limit condition on the $z = h$ line as with a computer model with very narrow partition walls. This also makes possible a comparison with the results valid in the computer model. However, sound propagation occurs parallel to the duct between the partition walls at least to a depth of $z = h'$ as with the model of the ladder network, so that at $z = h$ no locally active boundary can be assumed.

Calculation of the wave propagation in periodic structures is possible in principle if the field is described with three-dimensional partial waves. The applicability of this method, which is common for electromagnetic delay lines, to acoustic

wave guides has been studied by Mechel [5]. It supplies the desired propagation constant over one period in the duct generally from a system of transcendent equations. Mechel was able to produce the conversions for the velocities perpendicular to the wall for a comb structure without absorption material with the assumption of simple relationships. However, if the prerequisite of a locally active boundary is maintained, the results described only the effect of the tooth width. The effect of the chamber width in the case of very narrow partition walls as the teeth of the comb, such as occur with noise dampers, is not ascertained in this way.

The present study concerns the description of the boundary condition for a duct wall subdivided into broad chambers, taking into consideration coupling in the fields behind the wall and deduction of the propagation constant in the duct over one period which is about equal to the chamber width. To this end, special efforts are made to obtain explicit approximations.

2. The Absorber Divided into Chambers

2.1 Measurement of Wall Admittance

The question as to what extent a non-locally active duct boundary occurs in the case of a wall subdivided into chambers can be answered using measurement method to determine the local variation in admittance on the line $z = h$:

$$\frac{1}{W(x)} = \frac{v}{P} \quad (1)$$

For measuring wall resistances $W(x)$ in ducts with a noise field on which more precise data is not available, the usual methods fail which give the resistance from the reflection factor. Another method can be used, however, which from one measurement permits direct reading of the real and imaginary portion of the complex wall transmittance with respect to one

parameter.¹ The basis of the method is the relationship:

$$\frac{p''}{p} = \frac{1 + \frac{Z}{\rho c}}{1 - \frac{Z}{\rho c}} \quad (3)$$

which is valid with the following equation in a free sound field:

$$\Delta p = -\rho \frac{d^2 \phi}{dt^2} \quad (2)$$

With $p = |p|e^{j\phi}$, the splitting up into real and imaginary parts turns out to be:

$$\frac{d}{dx} (\ln |p|) = \frac{\omega}{c} \left| \frac{Z}{\rho c} \right| \quad (3a)$$

$$\frac{d\phi}{dx} = \frac{\omega}{c} \left| \frac{Z}{\rho c} \right| \quad (3b)$$

From this we can directly deduce measurement rules for the wall admittance multiplied by the angular velocity ω and the density of the gas ρ in front of a wall. If we measure the sound pressure level

$$L(x) = 20 \lg \frac{|p|}{p_0} \quad (4)$$

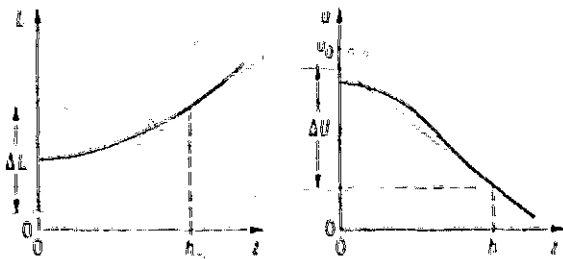
then the slope of the curve at point $x = h$ plotted along the line $x = x_0$ is:

$$\frac{dL}{dx} \Big|_{x=h} = 8.7 \frac{d}{dx} (\ln |p|)_{x=h} \text{ dB} \quad (5)$$

Plotting the level difference for the width $\Delta x = h$ according to 76

1. The method was also given by Mechel [6]. It also serves to measure the "noise radiation at the outlet opening of ducts." An article by the author of this paper [14] has been published on this and has led "to the development of a device for complex sound field measurements" [15].

the graph shown in Fig. 2 gives us:



$$\frac{\Delta L}{U_0} \approx \frac{h}{U_0} \frac{dL}{dz} \Big|_{x_0, h} = \operatorname{Im} \left\{ \frac{\omega g h}{U^*} \right\}. \quad (6)$$

The voltage on the sliding contact of the level recorder which records the level $L(x_0, z)$ is:

Fig. 2. Plot of the level gradient and phase gradient.

$$U = \frac{p}{|p|} U_0 e^{j\phi(x_0, z)} U_0. \quad (7)$$

If we form the difference with a fixed voltage $U_0 e^{j\phi_0}$, whose phase ϕ_0 is less than $\phi(x_0, h)$ then we obtain:

$$U = |e^{j(\phi - \phi_0)} - 1| U_0 \approx |j(\phi - \phi_0)| U_0 \quad (8)$$

in the vicinity of $z = h$. The slope of the voltage recorded with a linear recorder at the point $z = h$ is:

$$\frac{dU}{dz} \Big|_{x_0, h} = -U_0 \frac{d\phi}{dz} \Big|_{x_0, h} \quad (9)$$

For plotting purposes the voltage difference ΔU for the width $\Delta z = h$ is conveniently related to the voltage U_0 as per Fig. 2:

$$\frac{\Delta U}{U_0} \approx \frac{h}{U_0} \frac{dU}{dz} \Big|_{x_0, h} = \operatorname{Re} \left\{ \frac{\omega g h}{U^*} \right\}. \quad (10)$$

2.2 Examples

The practical execution of the measurement was carried out in a experimental setup as shown in Fig. 3. A duct with an inside

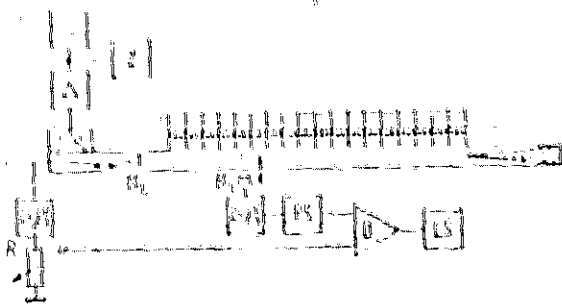


Fig. 3. Measurement arrangement for determining the local wall admittance in a duct lined with absorbent material.

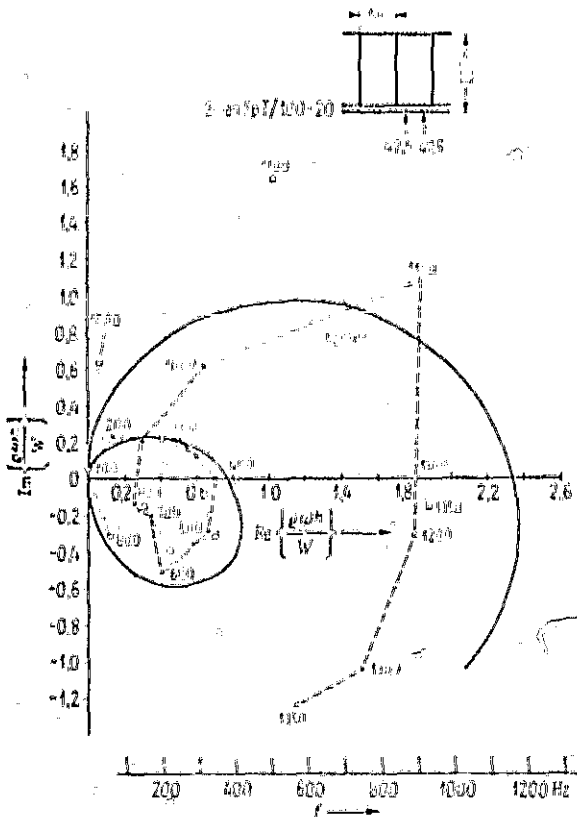
cross-section of $0.1 \text{ m} \times 0.25 \text{ m}$ was lined over a length of 1.8 m on a broad side with an absorber divided into compartments of width l . It was stimulated from one end with pure tones whose frequency was controlled with the meter Z . The opposite end was closed with a cover which was almost reflection-free for frequencies above 150 Hz .

The changes in sound pressure transverse to the axis of the duct were measured with a continuously adjustable probe tube connected to a one-inch condenser microphone M outside the duct. Because of the small inside diameter of the probe (3 mm), it was possible to scan the sound field in a pointwise fashion.

The level of the voltage given off by the microphone M_q was recorded after selective amplification via a terz [tertiary?] filter - analyzer with the sound recorder PS . To measure the phase a voltage proportional to the slide contact voltage of the sound recorder was applied to the differential amplifier D . The required reference voltage was provided by a second microphone M_1 , which was placed in the duct so it could be moved in the lengthwise direction in order to adjust a desired phase. The difference of the voltages adjusted to the same amplitudes with regulator R was recorded with the linear recorder LS .

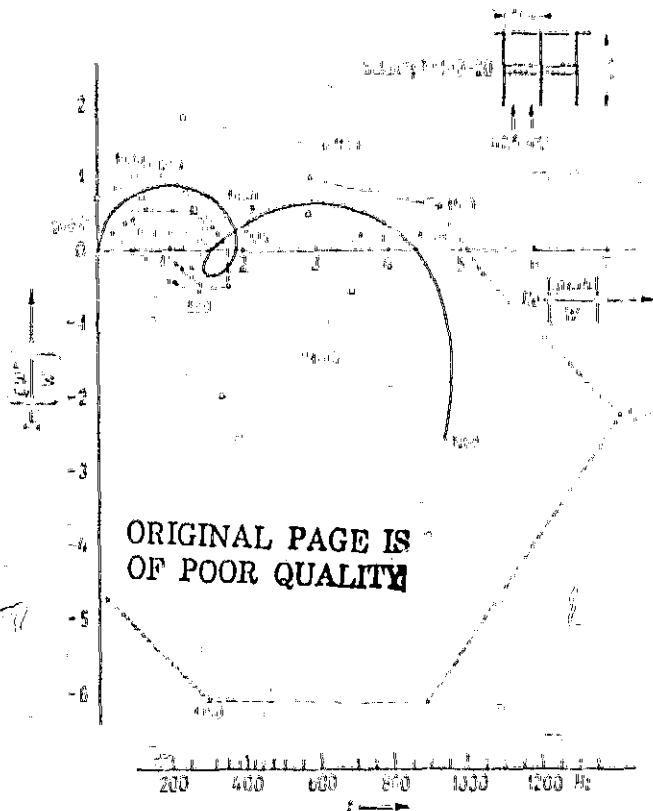
Measurements of wall admittances were carried out for various arrangements of a thin absorbent layer of Sillan SpT/100-20 whose flow resistance was determined to be $r' = 1$ first of all with parallel flow at about $r = 40 \text{ Rayl}$, i.e. with respect to the characteristic resistance of air. On one

side the layer of absorbent material, as shown in Fig. 3, was applied centrally in compartments 20 cm deep, and on the other side directly on the duct. The loci of sound and phase measurements are plotted in Figs. 4 and 5 on two lines symmetric with respect to the middle of a compartment of width $b = 10$ cm at distances $\Delta x = 42.5$ cm and $\Delta x = 47.5$ cm from the beginning of the absorber section. In comparison with the theoretical loci for wall admittances with perpendicular



Measurement points

Fig. 4. Loci of the normalized local wall admittance.
 X--X Measurement at $x = 42.5$ cm
 O--O Measurement at $x = 47.5$ cm
 — Calculation for perpendicular sound wave incidence and an absorbent layer with $r' = 1$.



Measurement points

Fig. 5. Loci of the normalized local wall admittance.
 X--X Measurement at $x = 42.5$ cm
 O--O Measurement at $x = 47.5$ cm
 — Calculation for perpendicular sound wave incidence and an absorbent layer with $r' = 1$.

sound wave incidence, the influence of the compartment width is obvious with strong local variations for the measured admittances.

A sound wave incidence amplified over the entire width of the compartment with respect to the average value in the section close to the transmitter is characterized by an increased real portion of the wall admittance. The sound wave already dampened on average by the duct up to the section of the compartment entrance away from the transmitter their allows an increased output of sound from the chamber into the duct so that the real portion of the wall admittance is reduced or even becomes negative.

2.3 Boundary Condition

177

The local variation in wall admittance in the case of a duct wall divided into compartments is a property on the one hand of the exciting sound field and, on the other, the geometry and material constants of a porous absorber in the compartment. In order to formulate a boundary condition, the effects of the excitation conditions have to be separated from the wall properties. This is possible with a mode representation with which the sound field in a compartment can be completely described. The propagation condition for each mode is given by its characteristic wave impedance. The interaction in each case of two opposing modes can be formulated at the compartment entrance as a boundary condition for the duct.

In the case of a rectangular compartment with hard partition walls divided by the interval b , the following mode equation is valid:

$$p(x,z) = \sum_{n=0}^{\infty} I_n \cos \frac{n\pi x}{b} h_n(z),$$

(11)

whence it follows with the standardization $f_v(h) = 1$ that:

$$p(x, h) = \sum_n J_n \cos \frac{n\pi x}{b} \quad (12)$$

If the sound pressure $p(x, h)$ is known only at m points in the compartment entrance, then the discrete Fourier synthesis with m clearly defined modes is to be used. Its representation with column vectors for the pressure distribution and mode amplitudes

$$\begin{pmatrix} p_{1,h} \\ \vdots \\ p_{m,h} \end{pmatrix} = P_h \quad (13)$$

$$\begin{pmatrix} A_0 \\ \vdots \\ A_{m-1} \end{pmatrix} = A \quad (14)$$

and with a coefficient matrix

$$C = \begin{pmatrix} 1 & \alpha_{11} & \dots & \alpha_{1,m-1} \\ \vdots & \vdots & & \vdots \\ 1 & \alpha_{m1} & \dots & \alpha_{m,m-1} \end{pmatrix}; \alpha_{in} = \cos \frac{n\pi x_i}{b} \quad (15)$$

gives the following equation in place of (12):

$$P_h = CA. \quad (16)$$

Conversion to mode analysis looks as follows:

$$A = C^{-1}P_h. \quad (17)$$

The inverse matrix C^{-1} is especially easy to form if the grid points at

$$x_n = \frac{2n-1}{2m} b \quad (18)$$

are equidistant and symmetrical to the duct walls. Essentially then we only have to form the transposed matrix of C to obtain the inverse matrix C^{-1} :

$$C^{-1} = \frac{2}{m} \begin{pmatrix} \frac{1}{2} & \dots & \frac{1}{2} \\ a_{11} & \dots & a_{1m} \\ \vdots & \dots & \vdots \\ a_{m,1} & \dots & a_{m,m} \end{pmatrix} \quad (19)$$

The mode expression (11) now leads to the formulation of a general boundary condition by which with the gradient formation

$$\frac{\partial p}{\partial z}(x, z) = p'(x, z) = \sum_{v=1}^m A_v \cos \frac{v\pi x}{b} j'_v(z) \quad (20)$$

and a definition, possible according to Eq. (3), of standardized admittances L_v for the modes at the compartment entrance

$$\frac{j'_v(h)}{j_v(h)} = \frac{j \omega \rho}{R_{v,h}} = \frac{L_v}{h} \quad (21)$$

the pressure gradient at each point x in front of a compartment is combined with the pressure curve, characterized by the mode amplitudes A_v , in front of an entire compartment-width:

$$-p'(x, h) = \frac{1}{h} \sum_{v=1}^m A_v L_v \cos \frac{v\pi x}{b} \quad (22)$$

By exclusively considering m pressure gradients at the point

$$P_k = \begin{pmatrix} p_{1,h} \\ \vdots \\ p_{m,h} \end{pmatrix} \quad (23)$$

ORIGINAL PAGE IS
OF POOR QUALITY

characterized by Eq. (18), only $m-1$ standardized wall admittances L_v of the higher modes can be determined, which are summarized as follows in a diagonal matrix:

$$L = \begin{pmatrix} L_1 & & \\ & \ddots & \\ & & L_{m-1} \end{pmatrix}. \quad (24)$$

In place of Eq. (22), the following boundary condition is then valid with Eq. (17):

$$P_L' = \frac{1}{h} C L C^{-1} P_L. \quad (25)$$

In connecting the pressures with the pressure gradients, a similarity transformation

$$C L C^{-1} = L_v \quad (26)$$

must be used on the admittance matrix L .

The standardized wall admittances L_v are clearly determined by the form of a compartment and the absorbent material in it. For example, the solution of the telegraphic equation

$$\frac{\partial^2 p}{\partial z^2} + k^2 p = 0 \quad (27)$$

for a rectangular compartment of depth d filled with a homogeneous but anisotropic absorbent material in which the wave numbers

$$k_v = k \begin{cases} k_z = \sqrt{k^2 - \omega^2 \epsilon_v} \\ k_z = j \sqrt{\omega^2 \epsilon_v - k^2} \end{cases} \quad (28)$$

are increased with respect to the wave number k in air due to structural factors of the absorption material χ_x or χ_z and becomes complex due to the length-specific resistances E_x and E_z , gives the standardized mode admittances: 29

$$L_x = \frac{h}{b} r_{\pi a} \frac{k^2}{k_p k_z} \left| 1 - \left(\frac{k_p h}{r_{\pi}} \right)^2 \right| \quad (29)$$

$$= \tanh \left| \frac{k_z d}{k_p b} r_{\pi} \right| \left| 1 - \left(\frac{k_p h}{r_{\pi}} \right)^2 \right|$$

The reaction of the hard end of the compartment is characterized by \tanh . It is negligible if the higher modes excited at the compartment entrance in narrow compartments fade away quickly. Then in the special case of isotropic absorbent material we obtain:

$$L_x = \frac{h}{b} r_{\pi} \frac{1}{\sigma - j \omega \rho} \quad (30)$$

In narrow compartments without absorbent material or with absorbent material in a depth in which the higher modes have already subsided, according to Eq. (30) $\frac{r_{\pi} h}{L_x b}$ is real and independent of frequency. By contrast, in narrow compartments with absorbent material $\frac{r_{\pi} h}{L_x b}$ becomes imaginary and proportional to frequency, i.e. at low frequencies it becomes much smaller according to the magnitude. Substantially greater values and a change in sign for L_x occur if modes are propagated as waves in wider compartments. Using measurement techniques it was possible to prove this behavior from the results plotted in Figs. 4 and 5 by eliminating the excitation conditions with the additional measurement of the sound pressure curve at the compartment entrance.

3. Solution of the Wave Equation in a Periodic Duct with Couplings in the Wall Lining

To calculate the sound propagation in a periodic duct in which the boundary condition (25) is valid for each section with regular partition walls in the wall lining, a periodic solution

$$p(x,z) = e^{i(\omega t - \gamma z)} p(x) \quad (31)$$

of the wave equation

$$\frac{\partial^2 p}{\partial x^2} + \frac{\partial^2 p}{\partial z^2} + k^2 p = 0 \quad (32)$$

is sought which gives the propagation constant γ as a function of the frequency, the dimensions of the rectangular duct and the standardized admittances of the compartment modes. In place of a solution which is possible in principle with the setting-up of partial waves which leads implicit representation with transcendental functions, a differential calculation adjusted to the discrete Fourier analysis of the limit values is used from which explicit approximations can be derived.

3.1 Two-dimensional Differential Approximation

Using differential calculus the continuum of the duct is broken up into individual elements, on the connecting points of

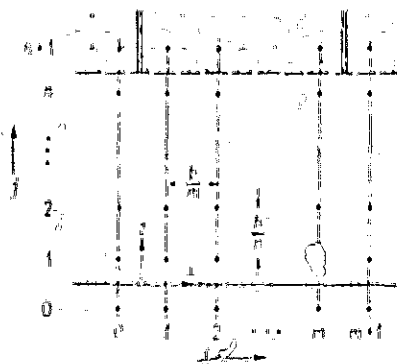


Fig. 6. Scanning field for differential calculation.

which the sound field is exclusively considered. As shown in Fig. 6, for this purpose the x, z plane of the duct is covered with a scanning field which subdivides the compartment width b , which is about equal to the period length l , into m sections and the duct width h

into n equal sections. In each scanning element with the dimensions $\Delta x = b/m$ and $\Delta z = h/n$ the differential quotient of wave equation (32) are approximated by central differential quotients. At points with the scanning coordinates i, j this gives the differential equation

$$p_{i,j} + \frac{1}{2}(p_{i-1,j} + p_{i+1,j}) + \frac{1}{2}(p_{i,j-1} + p_{i,j+1}) - p_{i,j} = 0. \quad (33)$$

wherein:

$$\alpha = \left(\frac{hm}{bn}\right)^2 \quad (34)$$

$$\beta = \left(\frac{lh}{n}\right)^2 \quad (35)$$

The differential equation is to be written down for all scanning points i, j which lie within a period of the solution range of the wave equation in the duct and on its boundary. For a clear representation, in accordance with Eq. (13) the pressures of a scanning line are combined with the number j into a column matrix P_j . The pressures outside the basis area are connected to the pressures within the period in question by two independent periodicity conditions

$$\begin{aligned} p_{0,j} &= e^{i\alpha} p_{m,j} \\ p_{m+1,j} &= e^{i\alpha} p_{1,j} \end{aligned} \quad (36)$$

in accordance with Eq. (31) with $l = b$. The matrix representation of the differential equation systems for all lines j looks as follows:

$$\begin{pmatrix} E & D & E \\ & \cdot & \cdot \\ & E & D & E \end{pmatrix} \begin{pmatrix} P_n \\ \vdots \\ P_1 \end{pmatrix} = 0. \quad (37)$$

In this arrangement E stands for the unit matrix and

$$D = \begin{pmatrix} \beta & \alpha & & \alpha e^h \\ \alpha & \beta & \alpha & \\ & & \ddots & \\ & & \alpha & \beta \\ \alpha e^{-h} & & \alpha & \beta \end{pmatrix} \quad (38)$$

The vectors P_0 and P_{n+1} comprise pressures outside the duct boundaries and are to be expressed using the boundary condition on the hard duct wall and the absorbent duct wall by vectors within the duct. With the scanning situation as shown in Fig. 6, the hard duct wall as a symmetry line determines the following relationship:

$$P_n = P_1 \quad (39)$$

On the absorbing wall the differential approximation of boundary condition (25) gives the following:

$$-P'_h = -\frac{n}{h}(P_{n+1} - P_n) = \frac{1}{h} L_T P_h \quad (40)$$

The boundary vector P_h which is not obtained directly using the differential method is formed from the arithmetic mean of the vectors adjacent to the boundary. Thus we obtain from Eq. (40):

$$P_{n+1} = \left[-E + 2 \left(E + \frac{1}{2n} L_T \right)^{-1} \right] P_n \quad (41)$$

With the elimination of P_0 and P_{n+1} we get the following homogeneous set of equations from Eq. (37):

$$\begin{pmatrix} D+E & E & & \\ E & D & E & \\ & & \ddots & \\ & & E & D & E \\ & & & E & D - E + 2 \left(E + \frac{1}{2n} L_T \right)^{-1} \end{pmatrix} \begin{pmatrix} P_1 \\ P_2 \\ \vdots \\ P_{n-1} \\ P_n \end{pmatrix} = 0 \quad (42)$$

The desired eigenvalues γb which are contained in the matrices D are given by the zero points of the coefficient determinant. Their continued fraction representation looks as follows:

$$\det \left\{ \begin{array}{c} \mathbf{D} - \mathbf{E} + 2 \left(\mathbf{E} + \frac{\mathbf{L}_T}{2n} \right)^{-1} \\ - [\mathbf{D} - [\mathbf{D} - \dots [\mathbf{D} + \mathbf{E}]^{-1} \dots]^{-1}]^{-1} \end{array} \right\} = 0. \quad (43)$$

A polynomial representation can be given if using

$$\det \left\{ \mathbf{U}'_n \left(\frac{\mathbf{D}}{2} \right) \begin{array}{ccccc} & & \mathbf{D} & \mathbf{E} & \\ & & \mathbf{E} & \mathbf{D} & \mathbf{E} \\ & & & & \ddots \\ & & & & \mathbf{E} & \mathbf{D} & \mathbf{E} \\ & & & & & \mathbf{E} & \mathbf{D} \end{array} \right\} \quad (44)$$

we define a polynomial U'_n of the $n-1$ degree for the determinant with $(n-1)$ lines. The coefficients of this polynomial are then equal to those of the function $U_n(x)/\pm\sqrt{1-x^2}$, whereby $U_n(x)$ is the Tschebyscheff function of the second kind of degree n [7], [8]. With definition (44), the eigenvalue determinant of Eq. (42) can be represented by

$$\det \left\{ \begin{array}{c} \mathbf{U}'_{n+1} \left(\frac{\mathbf{D}}{2} \right) - \mathbf{U}'_{n-1} \left(\frac{\mathbf{D}}{2} \right) + \\ + \left[\mathbf{U}'_n \left(\frac{\mathbf{D}}{2} \right) + \mathbf{U}'_{n-1} \left(\frac{\mathbf{D}}{2} \right) \right] 2 \left(\mathbf{E} + \frac{\mathbf{L}_T}{2n} \right)^{-1} \end{array} \right\} = 0, \quad (45a)$$

or by

$$\det \left\{ \sum_{r=0}^n \mathbf{D}^r \left[r, \mathbf{E} + s_r, 2 \left(\mathbf{E} + \frac{\mathbf{L}_T}{2n} \right)^{-1} \right] \right\} = 0, \quad (45b)$$

in which r_v and s_v are to be formed from the coefficients of the Tschebyscheff functions pertaining to Eq. (45a). The polynomial of the n th degree of D accordingly has many solutions $e^{\pm\gamma n b}$, of which in a long duct only the one with the smallest

amount of damping is interesting. The explicit solution for the thus characterized fundamental mode as a function of the boundary condition is only possible for small n 's, i.e. for a few intervals over the compartment width. However the accuracy of the results is good for ducts which are narrow in relation to the wavelengths and thus which are especially interesting for noise dampers.

3.2 Extension to the Homogeneous Duct Theory

In a duct on the absorbent wall of which no coupling occurs, the elements L_V of the admittance matrix are all equal. With Eqs. (21) and (26), the following relationship holds:

$$L_V = \frac{jkh \gamma^n}{n} B. \quad (46)$$

The period in the duct is b/m . The limit transition to an infinitesimal subdivision with $m \rightarrow \infty$ is equivalent to an interval subdivision with $m = 1$ and $b \rightarrow 0$. For $m = 1$ the matrix D deteriorates to:

$$D = 1 + 2 \cosh \gamma b. \quad (47)$$

In the limit transition $b \rightarrow 0$, with $\cosh \gamma b \approx 1 + 1/2(\gamma b)^2$ and the abbreviated terms (34) and (35), the following equation holds:

$$D = \left(\frac{kh}{n} \right)^2 + 2 + \left(\frac{\gamma b}{n} \right)^2. \quad (48)$$

Eq. (45a) to be used on simple numbers with Eqs. (46) and (48) gives the following implicit result known from Morese [9] and Cremer [10] in the limiting case $n \rightarrow \infty$:

$$\frac{j \omega \rho}{n} = \frac{1}{k^2 + \gamma^2} \tan(h \sqrt{k^2 + \gamma^2}). \quad (49)$$

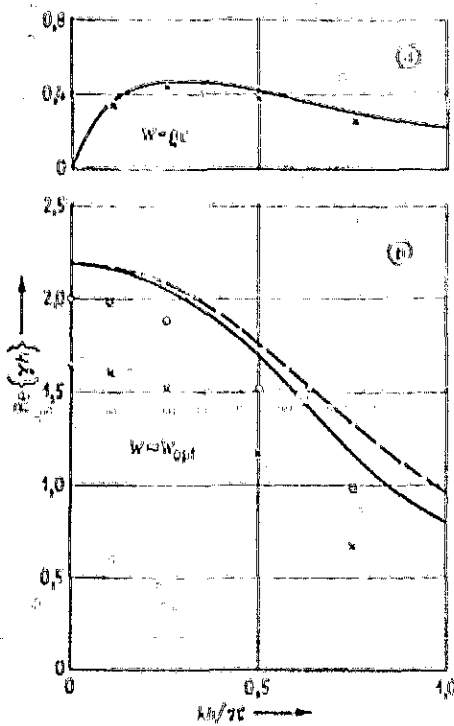


Fig. 7. Calculated values of the damping constant $Re\{\gamma h\}$ as a function of the frequency parameter kh/π .

(a) $W = \rho c$.

— Homogeneous wall, calculated values as per Eq. (50),

XXX in a wall subdivided into compartments of width $b = h$ without absorbent material at the compartment entrance

(b) $W = W_{opt}$.

— Homogeneous wall, calculated values as per Eq. (53),

--- Homogeneous wall, calculated values as per Eq. (54),

XXX in a wall subdivided into compartments of width $b = h$ without absorbent material at the compartment entrance, calculated values with W_0 as per Eq. (51),

000 Maximum damping $Re\{\gamma h\}_{max}$.

The damping constant in the form of the real portion of Eq. (53) is plotted in Fig. 7 in comparison with the damping constant for the optimum wall resistance according to Eq. (54). Only at higher frequencies or wider ducts does a small and restricted error occur.

The frequency response of the maximum damping in the homogeneous duct shows the quality of the differential approximation only in the extreme case, but it is important only for very narrow band noises. For wide band noises the relationship between the optimum wall resistance and frequency cannot be established [11]. In this case, larger wall resistances are more favorable for which, as an example, $W = \rho c$ is treated. Calculated values for this wall resistance are determined according to Eq. (50) and also shown in Fig. 7 in a frequency range in which simple approximations fail. In comparison with the values which can be read from the Morse and Cremer damping charts errors of less than 5% arise which are just less than the reading

accuracy. Thus the result given by Eq. (50) can be used in place of the damping chart drawn to evaluate Eq. (49) in all technically interesting cases if a numerical determination, with a computer, of the propagation constant as a function of the wall resistance requires and explicit representation.

3.3 Effect of Couplings in the Duct Wall

Initial information on the effect of the compartment width is given by plotting Eq. (43) for narrow ducts in which with a large wall resistance W_0 an almost flat, weakly damped sound field is present. Only $n = 1$ scanning line over the duct width and $m = 2$ scanning lines with narrow compartments have to be taken into account. For the familiar approximation equation of the propagation constant

$$r = jk \left[1 - j \frac{e^r}{W_0 k h} \right] \quad (55)$$

the calculation gives a correction factor:

$$1 - \frac{\pi b}{32 h} \left(\frac{l_1 b}{\pi h} \right) \quad (56a)$$

In the case of compartments without absorbent material at the entrance, for which $\frac{l_1 b}{\pi h} \approx 1$, the correction factor is almost in agreement with the result of a more rigorous calculation by Collin [12] for the analogous electrical problem. Collin gives a $\ln 2 / \pi$ -fold orifice correction for the compartment width b as an addition to the duct height h of a rectangular duct and an equivalent deduction from the compartment depth. This gives a damping reduction in the duct with the factor:

$$1 - \frac{\ln 2 b}{2\pi h} = 1 - \frac{\pi b}{32 h} \cdot 1.1. \quad (56b)$$

In addition to the good agreement of the numerical factor, (56a) also gives quantitative information on the effect of absorbent material in the compartment. L_1 is already very small with small losses at the compartment entrance, so that no correction factor has to be taken into account.

With only two reference lines over the compartment width an approximation for higher frequencies or wider compartments is no longer admissible. Nevertheless, qualitatively correct relationships are still evident in the vicinity of the first parallel resonance of the compartments at $kh = \pi$. There the duct damping, according to the approximation with $n = 1$ and $m = 2$, turns out to be proportional to the product $L_0 L_1$. If as a result of small losses in the compartments according to Eq. (29) L_1 becomes small, the sound propagation is only slightly damped. Compensation is possible by means of an especially large admittance L_0 . This has already been pointed out by Ingard and Pridmore-Brown [13] on the basis of experimental findings.

More exact calculated results for sound-absorbent wall linings were determined with a scanning field of $n = m = 2$ and are plotted in Fig. 7. Assuming that there is no absorption material at the entrance of the compartment, calculated values with a scanning form factor of $\alpha = 1$ for the wall resistance $W_0 = \rho c$ show an increasing reduction in the damping effect with increasing frequency in contrast to the case of the homogeneous duct wall. With the first parallel resonance in the compartment at $kh = \pi$, the damping is 0, if without absorption material the wall admittance of the only considered first upper mode is $L_1 = 0$.

The reduction in damping is even greater with the same scanning field in the vicinity of the optimum wall resistance. This is shown by calculated values in Fig. 7 for the wall

resistance W_0 according to Eq. (51) with unobstructed coupling at the compartment entrance. Taking into consideration a higher compartment mode, however, the route in Eq. (50) giving the difference between the bottom mode and top mode in the duct is changed so that the damping calculated with Eq. (51) no longer represents the maximum value. From the new zeropoint of the route a smaller optimal wall resistance W_0 with increasing coupling can be determined in which case the maximum damping in the duct established itself with a disappearing difference for the bottom mode and top mode. For maximum coupling at $L_1 = \pi$, the calculated values of $\text{Re} \{y_h\}_{\text{max}}$ to be sure lie below the curve for the homogeneous duct in Fig. 7, but not to the extent as is calculated in the neighborhood of the wall resistance using Eq. (52). Again a calculated result for the frequency parameter $kh/\pi = 1$ is not given, since there no damping is produced with $L_1 = 0$.

3.4 Examples

Numerical analysis of the differential calculation is performed on a small digital computer using a scanning field with $n = 2$ lines over the duct width h and $m = 4$ lines over the compartment width b for two technically interesting noise damping arrangements. The results are compared with measurements made in a duct as shown in Fig. 3 with the wall linings described in section 2.2.

Assuming local action of the wall linings, the propagation constant in the duct as per Eq. (50) is calculated as a function of the frequency parameter kh . The real portion or the damping $D_h = 8.7 \text{ Re } h \text{ dB}$ with respect to the length h is shown in Figs 8 and 9. They show characteristic damping maxima when the compartment depth d is an odd-numbered multiple of a quarter wavelength. The damping minimum occurring in Fig. 8 at the resonance of $\lambda/2$ is avoided in Fig. 9 by the absorbent material arrangement.

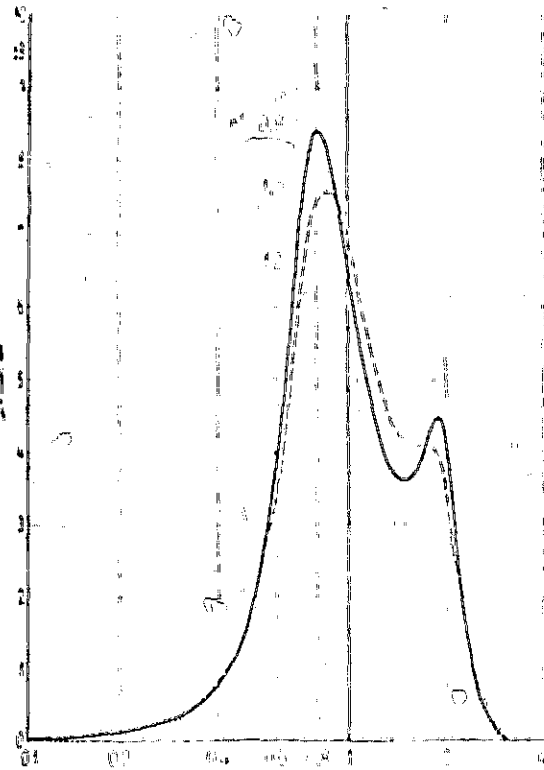
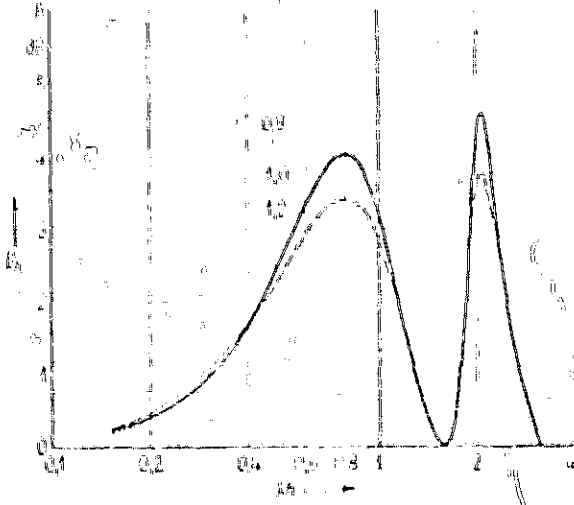
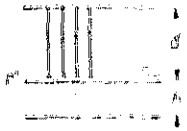
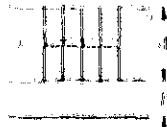


Fig. 8. Calculated values for duct damping $D_n = 8.7 \text{ Re}\{\gamma\} \text{ dB}$ as a function of the frequency parameter kh for different flow resistances r' and locally active duct walls.

Fig. 9. Calculated values for duct damping $D_n = 8.7 \text{ Re}\{\gamma\} \text{ dB}$ as a function of the frequency parameter kh for various flow resistances r' and locally active duct walls.

When comparing with measured values the strong dependency of the propagation constant on the exact value of the flow resistance of the absorbent material layer must be taken into account. As the calculated results plotted in Figs. 8 and 9 show, changes of as little as 20% have a considerable effect on r' at the compartment resonance frequency. In practice, such tolerances within a sample of absorption material must be taken into account.

183

Calculated results on the effect of the compartment width, which is taken into account by the propagation of three higher

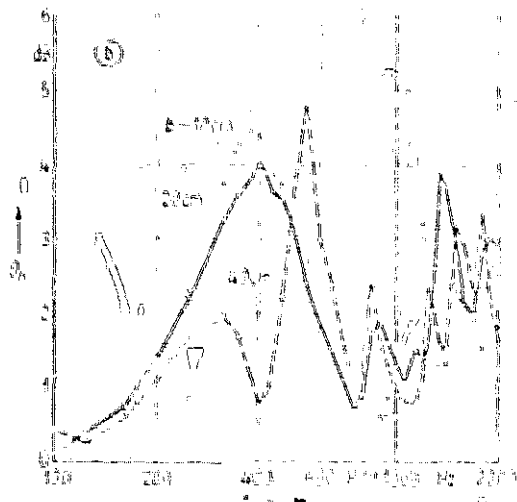
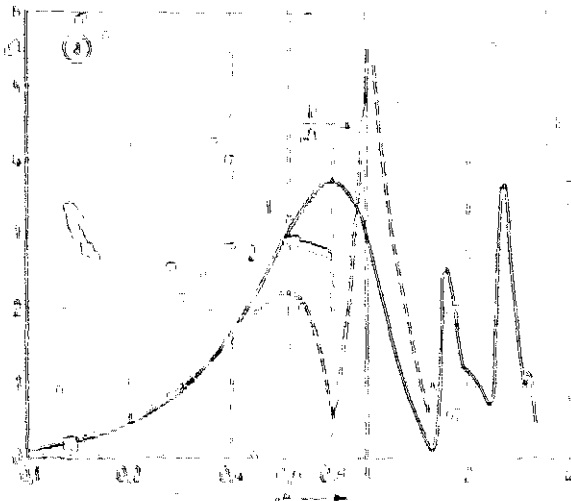


Fig. 10. Affect of the compartment width on duct damping D_n . (a) Calculated values as a function of the frequency parameter kh , (b) measured values as a function of the frequency f .

modes in the compartment, are plotted in Figs. 10a and 11a. As Fig. 11a shows, the effect without absorption material at the compartment entrance is already clearly noticeable at the first low resonance, even if the compartment width is still small with respect to the wavelength. By contrast, as Fig. 10a clearly shows, in the presence of more porous absorption material at the compartment entrance it first causes a reduction in damping only just below the first parallel resonance in the compartment.

The parallel resonances in the compartments have damping minima which with simultaneous antiresonance in the compartment depth are strongly pronounced, however in conjunction with a resonance they remain restricted to a narrow frequency range.

At higher frequencies, resonances of the upper mode in the compartment depth determine additional damping maxima. The frequency parameter of the first maximum is estimated using

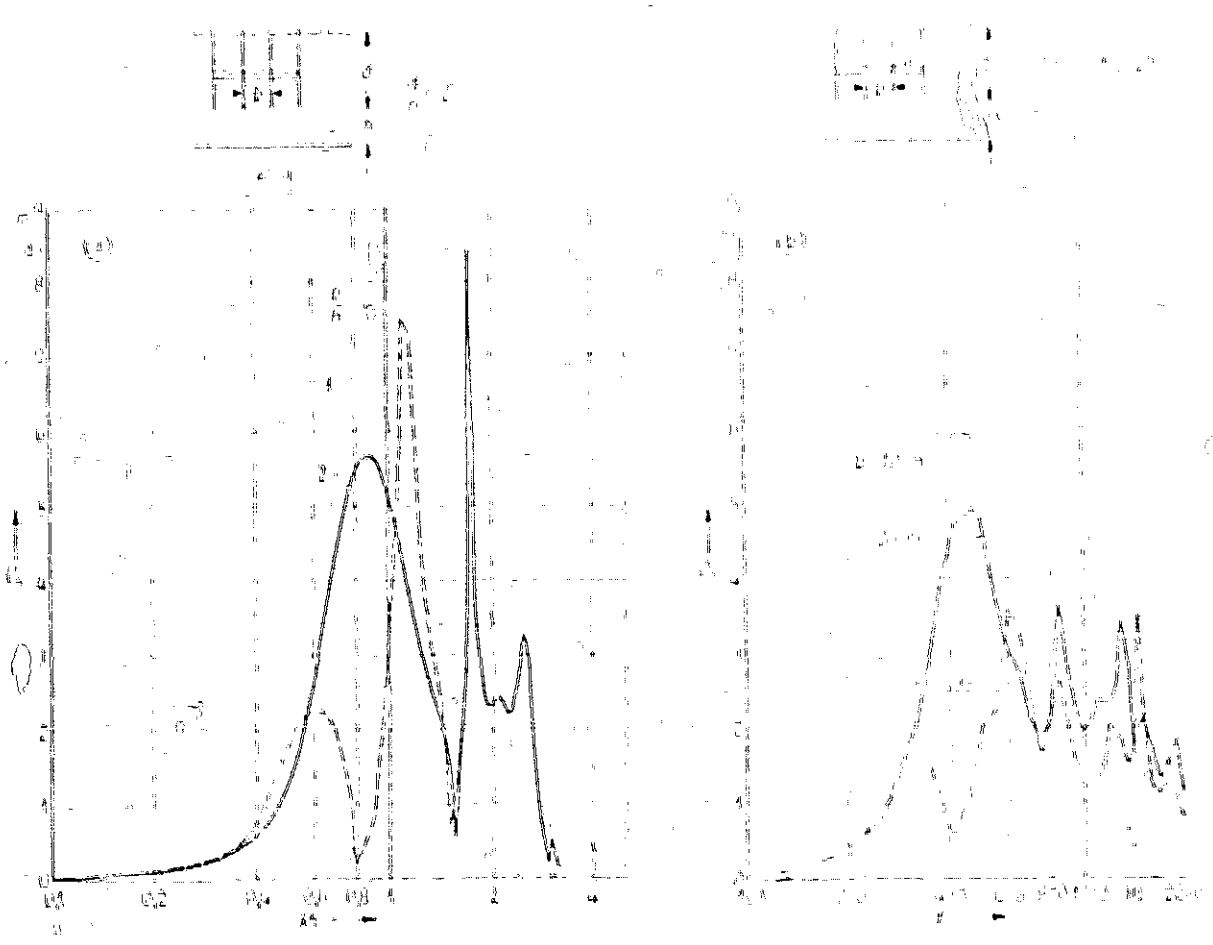


Fig. 11. Effect of the compartment width on the ducting damping D_h . (a) Calculated values as a function of the frequency parameter kh , (b) measured values as a function of the frequency f .

Eq. (29) from the condition:

$$\frac{\pi d}{b} \left| 1 - \left(\frac{b}{x} \right)^2 \right| = 1 \quad (57)$$

With $d/h = 2$ we obtain for $b/h = 4$ the frequency parameter $kh = \pi/4 \sqrt{2}$, for $b/h = 2$ the value $kh = \pi/4 \sqrt{5}$ and for $b/h = 1$ the value $kh = \pi/4 \sqrt{17}$.

84

Comparative measurements were carried out in a rectangular duct lined on one side with absorbent material with a width of $h = 10$ cm and a height of $H = 25$ cm for compartment widths of $b = 10, 20$ and 40 cm up to $f = 1400$ Hz. The measurements were made with pure tones and also with narrow band noises. In all of the arrangements the absorption material remained unchanged. Only occasionally it was removed from every other partition wall. The sound pressure level plotted in a dynamics range of 50 db had a strictly linear curve with deviations of less than 1 db from a straight line, as long as the higher compartment modes as near fields at the compartment entrance produced exponentially subsiding surface waves in the duct which no longer significantly affected the sound field on the microphone placed in the middle of the duct.

The measured results for the damping with respect to the duct width are shown in Figs. 10b and 11b. The quantitative agreement with the calculated values is satisfactory. Small deviations arise at low frequencies due to the duct cover which is not completely reflection-free and also at higher frequencies at which the 2-cm thickness of the absorbent layer has an effect. Otherwise, however, the effect of the periodic structure with the influence of transverse and longitudinal resonances of higher modes in the compartments turns out to be in agreement with the calculation. Only the extreme values limited to very narrow frequency bands in the damping curve appear less pronounced, which is to be attributed to small irregularities of the compartments and, at higher frequencies, especially to the finite thickness of the absorption material layer. Practically speaking, there the increased eigen frequency of the wide compartment, in comparison with the one-dimensionally active, narrow compartments, has a smoothing effect on the frequency response of the propagation constant. In comparison with the homogeneous duct, the reduced but wide band damping effect of the measurement example 185

with compartments having a width of $h = 20$ cm in Fig. 11 b makes the principle interesting, from a technical standpoint, of the absorption material arrangement in the form of a thin plate midway in the depth of the compartment.

I would like to thank Prof. L. Cremer, Ph.D. Eng., for his encouraging interest in this study.

Submitted August 8, 1966.

ORIGINAL PAGE IS
OF POOR QUALITY

REFERENCES

1. Cremer, L., Acustica 3, 249 (1953).
2. Morse, P.M. and U. Ingard, Theoretical Acoustics, McGraw-Hill Book Co. Inc., New York 1968, p. 490.
3. Davis Jr., D.D., G.M. Stokes, D. Moore and G.L. Stevens Jr., NACA Rep. 1192 (1954).
4. Collin, R.E., Field Theory of Guided Waves, McGraw-Hill Book Co., Inc., New York, 1960 p. 375 ff.
5. Mechel, F., Acustica 16, 98 (1965/66).
6. Mechel, F., Verhandl. Deutsche Phys. Gesellsch (VI) 3, 391 (1968).
7. Klein, W., "Tschebyscheff functions," in C. Rint, Handbuch für Hochfrequenz- und Elektrotechniker [Handbook for High Frequency Engineers and Electrical Engineers], Vol. 3, Verlag für Radio-Foto-Kinotechnik GmbH [Publisher for Radio, Photography and Cinemagraphic Techniques], Berlin-Borsigwalde, 1957, pp. 146 ff.
8. Doetsch, G., "Functional transformations," in Sauer-Szabo, Mathematische Hilfsmittel des Ingenieurs. [Mathematical Aids for the Engineer], Part I, Springer Verlag, Berlin-Heidelberg-New York, 1967, pp. 421 ff.
9. Morse, P.M., J. Acoust. Soc. Amer. II, 205 (1939).
10. Cremer, L., Akust. Z. 5, 57 (1940).
11. Kurze, U., Acustica 15, 139 (1965).
12. Collin, R.E., see [4], p. 438.
13. Ingard, U and Pridmore-Brown, D., J. Acoust. Soc. Amer. 23, 589 (1951).
14. Kruze, U., Acustica 20, 253 (1968).
15. Kruze, U., Acustica 20, 208 (1968).